Environ Monit Assess (2008) 140:15–32
DOI 10.1007/s10661-007-9843-7

Invasive species change detection using artificial neural networks and CASI hyperspectral imagery

Ruiliang Pu · Peng Gong · Yong Tian · Xin Miao · Raymond I. Carruthers · Gerald L. Anderson

Received: 16 January 2007 / Accepted: 18 May 2007 / Published online: 28 June 2007

Abstract For monitoring and controlling the extent and intensity of an invasive species, a direct multidate image classification method was applied in invasive species (salt cedar) change detection in the study area of Lovelock, Nevada. With multidate Compact Airborne Spectrographic Imager (CASI) hyperspectral data sets, two types of hyperspectral CASI input data and two classifiers have been examined and compared for mapping and monitoring the salt cedar change. The two types of input data are all two-date original CASI bands and 12 principal component images (PCs) derived from the two-date CASI images. The two classifiers are an artificial neural network (ANN) and linear discriminant analysis (LDA). The experimental results indicate that (1) the direct multitemporal image classification method applied in land cover change detection is feasible either with original CASI bands or PCs, but a better accuracy was obtained from the CASI PCA transformed data; (2) with the same inputs of 12 PCs, the ANN outperforms the LDA due to the ANN's non-linear property and ability of handling data without a prerequisite of a certain distribution of the analysis data.

Keywords CASI data · Invasive species · Salt cedar · Change detection · ANN · LDA

Introduction

Because of natural and anthropogenic processes, Earth's surface features frequently change their state at a range of spatial and temporal scales (Aplin 2006).

R. Pu (✉)
Department of Geography, University of South Florida,
4202 E. Fowler Ave., NES 107,
Tampa, FL 33620, USA
e-mail: rpu@cas.usf.edu

P. Gong
Center for Assessment & Monitoring of Forest & Environmental Resources (CAMFER),
University of California, 137 Mulford Hall,
Berkeley, CA 94720-3114, USA

Y. Tian
Environmental, Earth and Ocean Sciences Department,
University of Massachusetts-Boston, 100 Morrissey Blvd,
Boston, MA 02125, USA

X. Miao
Department of Geography, Geology & Planning,
Missouri State University, 901 South National Avenue,
Springfield, MO 65897, USA

R. I. Carruthers
USDA, Agricultural Research Service,
Western Regional Research Center,
800 Buchanan Street,
Albany, CA 94710, USA

G. L. Anderson
USDA, Agricultural Research Service,
1500 N. Central Ave.,
Sidney, MT 59270, USA

Therefore, timely and accurate change detection of Earth's surface features provides us with the foundation of understanding relationships and interactions between human and natural phenomena to better manage and use resources (Lu et al. 2004). Introduction of exotic species and invasive species may cause change of land cover types in a terrestrial ecosystem. Such a change usually has negative impacts on ecological functions of natural ecosystems at various scales and becomes a serious problem to environment-friendly sustainable ecosystems all over the world (Jackson et al. 2002; Mack et al. 2000; Simberloff 2001). According to USDA ARS (2005) and Johnson et al. (2005), Salt cedars (*Tamarix chinensis*, *T. ramosissima*, and *T. parvifolia*) are invasive, shrubby trees that are rapidly colonizing riparian areas in Nevada and many other states in the United States (Johnson et al. 2005). *Tamarix ramosissima* is the principal invader that has contributed to significant reductions in beneficial vegetation, such as willows, cottonwoods and other plants crucial to agriculture and the natural environment. Salt cedars degrade various ecosystems, resulting in loss of millions of dollars per year in the U.S. (Johnson et al. 2005; USDA ARS 2005). Therefore, monitoring the invaded extent of the invasive species and controlling its corresponding spread across invaded areas is an important task.

Remote sensing techniques, especially hyperspectral remote sensing, have potential for mapping and monitoring of both degree and extent of invasion (Lass et al. 2002; Miao et al. 2006; Pu et al. 2007a; Underwood et al. 2003; Ustin et al. 2001). Hyperspectral data, with their sufficient spectral information, are expected to offer a great promise in mapping the abundance of particular species over a large area. In our previous work, we have tested the ability of hyperspectral data for mapping and monitoring the extent of an invasive species, salt cedar (Pu et al. 2007a) using the post-classification and normalized difference vegetation index (NDVI) differencing change detection methods. In the post-classification strategy, a principal component analysis (PCA) was separately performed to single-date Compact Airborne Spectrographic Imager (CASI) imagery in the visible bands and NIR bands. The PCA transformation first performed on the single-date image is not only for reducing the dimension of the hyperspectral data but for retaining most hyperspectral information. A complete matrix of change information and change/no-change maps were produced by overlaying two single-date classification maps, produced by using a maximum likelihood classifier (MLC) with inputs of PCs of the CASI data. In the NDVI differencing strategy, a linear regression model was developed between two NDVI images to normalize spectral differences caused by factors not related to land cover change. The NDVI differencing image was further processed with thresholds into change/no-change of salt cedar. By testing the single-date classification results and validating the change/no-change results, both change detection results have indicated that CASI hyperspectral data have a potential of mapping and monitoring the change of salt cedar. However, the accuracies of change/no-change results were not desirable enough yet. Therefore, it is necessary to continue to test some alternative methods for improving mapping and monitoring the extent of invasive species with the CASI hyperspectral data.

In this study, from a dozen of change detection techniques (Coppin et al. 2004; Gong and Xu 2004; Lu et al. 2004), an alternative method based on simultaneous analysis of multi-date images was adopted to directly classify multitemporal data into change/no-change classes (e.g., Liu and Lathrop 2002; Nemmour and Chibani 2006). This type of methods is described as spectral-temporal combined analysis (Lu et al. 2004) or direct multi-date classification (Gong and Xu 2004). Functionally, this method puts multi-date data into a single file then classifies the combined dataset and identifies and labels the change classes. One significant property is that this method allows us to obtain more complete information about land cover change than some post-classification methods (e.g., Khan 2005; Pu et al. 2007a). However, since the number of 'from-to' change classes in this method could be exponentially greater than those in a single date classification, it might be difficult to identify and label the change classes. Therefore this method is rarely applied in change detection practice. So far, there are fewer studies using this method in change detection, such as work of Civco et al. (2002), Liu and Lathrop (2002), Seto and Liu (2003) and Nemmour and Chibani (2006) for land use and land cover change detection. The reasons we adopted it in this land cover change detection analysis are that (1) this method can provide us with complete information about 'from-to' land

cover change, (2) so far, this approach was tested only with multispectral data such as Landsat Thematic Mapper (TM; e.g., Liu and Lathrop 2002) and Satellite Probatoire d'Observation de la Terre (SPOT) high resolution visible image (HRV) (e.g., Nemmour and Chibani 2006) rather than testing with hyperspectral data, and (3) the performance in change detection with this method was not fully evaluated.

Usually, such a direct multi-date classification method is executed with some conventional classifiers, such as MLC and minimum distance. In this invasive species change analysis, we would use an artificial neural network (ANN) algorithm in change detection because a few of successful application cases of ANN demonstrated its potential (e.g., Seto and Liu 2003; Sunar Erbek et al. 2004) with multispectral Landsat data. This is based on (1) the non-linear property of the ANN, which may more reasonably describe the possible non-linear characteristic of 'from-to' land cover change than a linear algorithm can (Gopal and Woodcock 1996), (2) in contrast with traditional methods, the ANN is a free distribution machine, which is also more tolerant to noise, turbidity factors as well as missed data (Nemmour and Chibani 2006), for instance, some remotely sensed data after transformation processing may result in non-normal distribution, (3) usually, a sample size for training the ANN classifier to achieve a satisfactory result is much smaller than that required by a traditional method (e.g., MLC; Foody et al. 1995), and (4) the ANN is capable of catching subtle spectral information from hyperspectral data for change detection and classification (Gong et al. 1997). After reviewing previous studies in change detection, a few of researchers indeed had successfully applied the ANN in different kinds of change detection, including either 'from-to' categorical change or continuous change. For example, Nemmour and Chibani (2006) used a fuzzy neural network (FNN) architecture for land cover change detection in a region of Algeria with the multitemporal SPOT HRV images and concluded the FNN based model giving out the best performance. In urban land use/land cover change detection with two TM images of a region acquired on different dates, Liu and Lathrop (2002) applied an ANN to classify the image data into 'from-to' classes. Their experimental results suggest the practical value of ANN-based change detection. Abuelgasim et al. (1999) also used FNN with multitemporal TM data acquired before and after the Gulf War to detect continuous change of land cover, caused by the Gulf War. They demonstrated that the FNN method outperformed MLC and K-means traditional methods. In remote sensing of forest change due to a prolonged drought in the Lake Tahoe Basin in California, Gopal and Woodcock (1996) successfully applied ANN with multitemporal TM images to predict magnitude of forest mortality. The results of their study indicate that the ANN estimates conifer mortality more accurately than the other approaches such as the Gramm–Schmidt technique. In short, all of the aforementioned researchers found that the ANN or FNN are very effective techniques in land cover and forest change detection, especially in detecting continuous change and providing with 'from-to' complete change information with the direct multi-date classification method.

In this study, we proposed using the direct multi-date classification change detection technique and ANN algorithm with the CASI hyperspectral data for detecting and monitoring the invasive species change. To evaluate the performance of ANN, we also tested a traditional method: Linear discriminant analysis (LDA). More specifically, our experimental objectives in this study include: (1) testing and evaluating the effectiveness of the direct multi-date classification method in salt cedar change detection with either all original CASI bands or principal component transformed data of the CASI imagery, and (2) comparing the performance of ANN and LDA classification techniques for analyzing land cover changes with the multi-date CASI data.

Study site and data set

Study site

Figure 1 presents the location of the study site that is located nearby Humboldt River, Lovelock, Nevada, USA (118°31′24″W, 40°01′13″N). In 2001, this study site was one of the sites chosen by USDA-ARS (United States Department of Agriculture, Agricultural Research Service), Western Regional Research Center for a project of bio-controlling the spread of the invasive species (salt cedar; Johnson et al. 2005; USDA ARS 2005). The center released beetles (leaf beetles) introduced from XinJiang, China at these

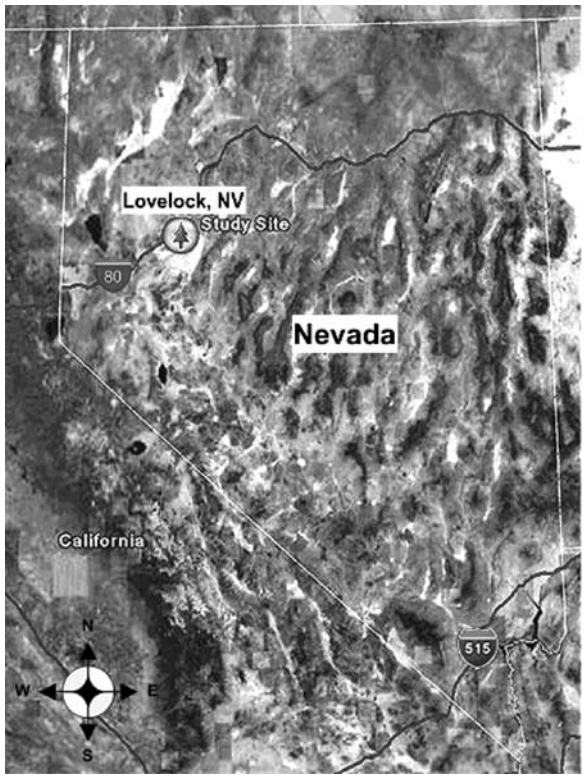

Fig. 1 An image map showing the location of the study site in Nevada, U.S.A.

sites. To monitor and evaluate the effectiveness of the bio-controlling measure in the area, USDA has flied CASI imagery several times yearly, depending on the stages of beetle growth, since beginning the project. The study area generally is flat. The major plant species is salt cedar that distributes mainly along the river with fewer non-dominant species such as willows and cottonwoods, etc.

In the study area, there exist the phonological changes of salt cedar July through September, reflecting in two image-pairs: JUL02–AUG02 and AUG02–SEP03. The NDVI change has proved the effect of phenological changes of vegetation (dominant salt cedar in the study area) on image spectra between the two different dates. For NDVI image-pair JUL02–AUG02, the NDVI for the unchanged pixels increases, reflecting on 1.11 slope coefficient of JUL02 related to AUG02. For NDVI image-pair AUG02–SEP03, the NDVI for the unchanged pixels decreases due to plant/crop beginning senescence and dried weather, reflecting on 0.83 slope coefficient of AUG02 related to SEP03. However, for NDVI image-pair JUL02–SEP03, the effect of phenology on NDVI image is not significant. Such phenomena of the phonological changes of salt cedar in the study area can help analyze the change detection results derived from multidate hyperspectral CASI data.

CASI imagery

The three-date CASI images, collected by the USDA-ARS (Sidney, MT) were used for mapping and monitoring the change of salt cedar after taking the bio-controlling measure. Some concise characteristics of the three-date CASI images are summarized in Pu et al. (2007a). Here we briefly describe the characteristics of the three-date CASI data again. The CASI data acquired on July 2, 2002 was with 2 m spatial resolution and 48 spectral bands of approximately 11 nm (hereafter referred to as JUL02); the CASI data acquired on August 29, 2002 was with 1 m spatial resolution and 36 spectral bands of approximately 15 nm (hereafter referred to as AUG02); and the CASI data acquired on September 10, 2003 was with 1 m spatial resolution and 32 spectral bands of approximately 17 nm (hereafter referred to as SEP03). The three-date images have different average bandwidth, spatial resolution and number of bands. With the direct multi-date classification method, the differences of average bandwidth and number of bands between the three-date CASI data can be overcome when an appropriate 'from-to' training/test sample set is first determined between two-date images (an image-pair). However, the spatial resolution difference needs to be solved through resampling and registration between the three-date images. Figure 2 shows the standard pseudo-color composite images of JUL02, AUG02 and SEP03. On the images, salt cedar appears in red, bare/wildland in blue–white and farmland in yellow–gray–blue. It is obvious that salt cedar areas in red distribute more on AUG02 than those on the other two CASI images.

Some field observation data and *in situ* measurements were taken during the field trips in June and July 2003–04. Digital photos were taken from different targets at different times, presenting the structure of landscapes and vegetation distribution and change. Spectrometer measurements were also taken from healthy leaves, damage leaves by beetles, and trunks of salt cedar at branch level as well as other typical land cover types with an ASD spectrometer (Analytical Spectral Devices, Inc., USA).

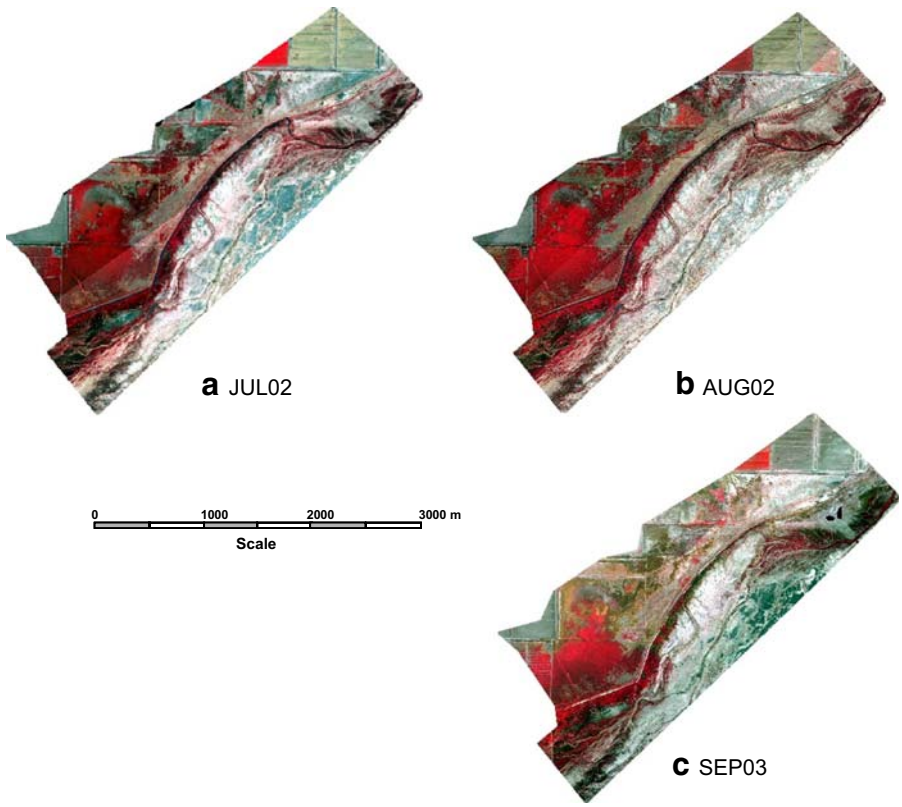

Fig. 2 Standard pseudo-color composite images of **a** JUL02, **b** AUG02 and **c** SEP03. On the images, *red areas* represent salt cedar

Twenty spectral samples were taken for each of these classes, and then they were averaged to represent the corresponding spectral signatures. Those filed-taken digital photos and spectral measurements were used to assist in selecting training, test and validation samples (directly reflecting 'from-to' land cover change) from the study area and in analyzing spectral difference between various land cover types and between different damage stages by beetles on the CASI imagery.

Methodology

Data pre-processing

The raw CASI images were first pre-processed, including mosaicking, resampling and geo-registration among the three-date CASI images before further analysis. CASI images of each date covering the study area consist of several image strips and need to mosaic together. Mosaicking was processed by using PCI/OrthoEngine (PCI Geomatics, Canada, 2003). Precise image registration is critical for change detection with multidate images. Registration was conducted among the three-date images by using SEP03 as a master image.

To efficiently apply the direct multi-date image classification method in this change detection with the CASI hyperspectral data, a principal component analysis (PCA) is used to transform the CASI data to reduce its dimension. To maximize available information obtained from the lower variability data in the visible region relative to the higher variability in the NIR region (Pu et al. 2007a, b), extraction of PCs from VIS and NIR regions is separately executed. This is because the available information from the visible region is more helpful for classification than the information from the NIR region, especially for identifying different vegetation types (Gong et al. 1997; van Aardt and Wynne 2001). Therefore, we applied PCA on 25 bands in the VIS region (420–705 nm) and on 23 bands in the NIR region (705–970 nm) for the JUL02 CASI data. Similarly, it was 19 bands in the VIS region (420–700 nm) and 17 bands in the NIR region (700–960 nm) for the AUG02 CASI data. For the SEP03 CASI data, it was 17 bands in the VIS region (421–

700 nm) and 15 bands in the NIR region (700–960 nm). A total of six principal component images (PCs; three from the VIS region and three from the NIR region) were extracted for each date. To emphasize on the variation of vegetation information, all PCA transform matrices (covariance matrices) in the study area were constructed with all NDVI pixel values >0.1. Table 1 presents the cumulative contribution rate of the first three PCs for each VIS and NIR region, calculated from the SEP03 CASI imagery, which indicates the first three PCs can almost account for the total variance of the imagery each of the spectral regions with an emphasis on vegetation variation.

Determination of samples

Given the advantage of providing 'from-to' complete change information with the direct multi-date image classification in change detection, it challenges us to define a set of training, test and validation samples used for efficiently performing the change detection task. Based on the objectives of this study (more focusing on the change of an invasive species: salt cedar) and the actual distribution of major land cover types in the study area, three known land cover types: Salt cedar (S), Farmland (F) and Bare/wildland (B), were first determined on the three individual images. Theoretically, there are nine 'from-to' change classes (three types × three types = nine classes) between any two dates. However, practically, according to our field observation, five 'from-to' change classes are high possible to occur in the study area (Table 2).

Table 1 Eigenvalue and cumulative contribution rate of PCA, calculated from the SEP03 CASI imagery

Eigenchannel	Eigenvalue	Variance (%)	Cumulat. cont. (%)
Three PCs from CASI visible bands			
1	42,985,320.00	96.08	96.08
2	999,356.60	2.23	98.31
3	623,947.30	1.39	99.70
Three PCs from CASI NIR bands			
1	26,029,240.00	94.81	94.81
2	833,488.00	3.04	97.85
3	375,712.90	1.37	99.22

Cumulat. cont. Cumulative contribution

To correctly delineate the five classes of training/test/validation samples/areas on the two-date combined images (either all original CASI bands or 12 PCs images), the three-date individual false color composite images were made and digital photos in the field in June and July of 2003–04 were collected; then referring to the digital photos and visual interpretation features on the false composite images (salt cedar in red, bare/wildland in blue–white and farm land with regular geometric forms in yellow–gray–blue) the training/test/validation samples/areas were delineated for each image-pair of the three-date CASI data: JUL02–AUG02, AUG02–SEP03, and JUL02–SEP03; finally, the delineated areas/samples of salt cedar and bare/wildland were further 'purified' with corresponding NDVI value range for individual images at different dates to remove those pixels/samples mostly off three-time standard deviation from individual class means. For instance, NDVI ranges for salt cedar are 0.3–0.6 for both JUL02 and SEP03 and 0.3–0.7 for AUG02, and NDVI ranges for bare/wildland are <−0.1 for both JUL02 and SEP03 and <0.0 for AUG02. The farmland type is easy and directly delineated on the false color images (Fig. 2). The final 'from-to' change classes are listed in Table 3.

Classification methods

A feed-forward artificial neural network (ANN) algorithm is used for classifying the 'from-to' land cover change classes in this invasive species salt cedar change analysis. The network training mechanism is an error-propagation algorithm (Pao 1989; Rumelhart et al. 1986). A neural network program developed by Pao (1989) has been adapted and used in this study. In a layered structure, as extensively used, the input to each node is the sum of the weighted outputs of the nodes in the prior layer, except for the nodes in the input layer, which are connected to the input features, i.e., digital numbers (DNs) of original CASI bands of the two-date images or 12 PCs (three PCs from VIS region and three PCs from NIR region of the CASI imagery at the first date and corresponding six PCs from the second date imagery) of an image-pair in this study. The nodes in the last layer output a vector of 5 'from-to' change classes, i.e., 'S to S', 'F to F', 'B to B', 'S to B', and 'B to S' classes (Table 2). One layer between the input and output layers is usually sufficient for most

Table 2 Notes on land cover changes between the three dates in the study area

Change direction	Note
$S_1 \rightarrow S_2$[a]	Salt cedar no change from T1 to T2, high possible
$S_1 \rightarrow B_2$[a]	Salt cedar changed to bare/wildland from T1 to T2, mostly killed by beetles, very possible
$S_1 \rightarrow F_2$[a]	Salt cedar changed to farmland from T1 to T2, not possible during the 14 months
$B_1 \rightarrow S_2$[a]	Bare/wildland changed to salt cedar from T1 to T2, mostly growing back after attacked by beetles
$B_1 \rightarrow B_2$[a]	Bare/wildland no change from T1 to T2, high possible
$B_1 \rightarrow F_2$[a]	Bare/wildland changed to farmland from T1 to T2, not possible during the 14 months
$F_1 \rightarrow S_2$[a]	Farmland changed to salt cedar from T1 to T2, not possible during the 14 months
$F_1 \rightarrow B_2$[a]	Farmland changed to bare/wildland from T1 to T2, not possible during the 14 months
$F_1 \rightarrow F_2$[a]	Farmland no change from T1 to T2, high possible

[a] There are five very possible change directions (classes). B1, F1 and S1 represent bare/wildland, farmland and salt cedar at time 1 (T1) while B2, F2 and S2 represent corresponding cover types at time 2 (T2).

learning purposes. The learning procedure is controlled by a learning rate (η), a momentum coefficient (α) and a number of nodes in the hidden layer (*h1*) that need to be specified empirically based on the results of a limited number of tests. The network training is done by repeatedly presenting training samples (pixels) with known 'from-to' change classes. Network training is terminated when the network output meets a minimum error criterion or optimal test accuracy is achieved. The trained network can then be used to predict the pixel-based 'from-to' change classes for each image-pair of the three-date CASI data. Finally, a validation sample set is used to verify and assess the classification accuracy of the multi-temporal hyperspectral data.

A linear discriminant analysis (LDA) classifier was also used to classify the 'from-to' change classes with inputs of 12 PCs of each CASI image-pair to compare with the classified results by ANN. The procedure DISCRIM in the SAS system (SAS Institute 1991) was used.

Table 3 Summary of samples (pixels) used for training, testing and validating ANN and LDA, extracted from all original CASI bands or principal component images

Image-pair	From-to	Training samples[a]	Test samples[a]	Validation samples
JUL02–AUG02	Salt cedar→salt cedar	208	416	563,175
	Farmland→farmland	207	414	241,947
	Bare/wild→bare/wild	209	418	439,504
	Salt cedar→bare/wild	220	440	19,770
	Bare/wild→salt cedar	228	456	40,953
AUG02–SEP03	Salt cedar→salt cedar	204	408	417,071
	Farmland→farmland	207	414	244,565
	Bare/wild→bare/wild	210	420	314,542
	Salt cedar→bare/wild	225	450	74,163
	Bare/wild→salt cedar	208	416	43,777
JUL02–SEP03	Salt cedar→salt cedar	203	406	359,777
	Farmland→farmland	207	414	242,534
	Bare/wild→bare/wild	202	404	405,317
	Salt cedar→bare/wild	212	424	25,498
	Bare/wild→salt cedar	212	424	25,411

JUL02–CASI Imagery acquired on July 2, 2002; *AUG02–CASI* imagery acquired on August 29, 2002; and *SEP03-CASI* imagery acquired on September 10, 2003

[a] Training and test samples separated strategy: First separate a dataset randomly into three subsets, then when 1st subset is used as training set, second and third as test set; when second subset as training set, first and third as test set; and when third as training set, first two subsets as test set. The numbers shown in the table are one third as training set and remaining two thirds as test set.

Accuracy assessment

In this study, three sets of samples were first determined: Training, test and validation. Total 3216, 3162 and 3108 of samples, corresponding to JUL02–AUG02, AUG02–SEP03, and JUL02–SEP03, respectively, were extracted for training and test uses. The samples of each paired image were separated into 1/3 as training and remaining 2/3 as test samples. Repeat this procedure three times (see Table 3). The training samples are used training ANN and LDA while test samples are used to evaluate the 'from-to' change class accuracies, generated with ANN and LDA. The Kappa and overall average accuracy (OAA; Congalton and Mead 1983; Congalton et al. 1983; Fung and LeDrew 1988; Foody 2002; Hayes and Sader 2001) calculated from test samples are used as indicators of evaluation results. In addition, to evaluate the performance of ANN and LDA in this invasive species change detection with the direct multi-date image classification method, a large set of validation samples (Table 3) is used to validate the classification maps. Again, the Kappa and OAA are used as indicators of the classifiers' performance.

Results and analysis

In registration, SEP03 was used as a master image while JUL02 (with 1.98 m RMSE) and AUG02 (with 1.79 m RMSE) as slave images. The registration errors (RMSE) were estimated based on 12–14 GCPs. The JUL02 was first resampled to 1 m pixel before the registration with a master image SEP03. In consideration of the CASI images with high spatial resolution and the no-random distribution of salt cedar along the stream, we thought that the RMSE of 1–2 m is acceptable. After the three-date images were mosaicked and geo-registered, the 'from-to' change classes were generated using the ANN and LDA classifiers with the multidate CASI data.

Determination of ANN structure

As mentioned before, a three-layer ANN structure was adopted. To train and test the ANN for classifying the multi-date image, the initial weight coefficients were given with computer-generated random numbers divided by a power function (e.g., 2^{15}; Pao 1989), and input CASI data (in both original DNs and PC images) were first normalized to the range of [0, 1]. When using two-date original CASI bands, 84 bands (48+36) for JUL02–AUG02, 68 input bands (36+32) for AUG02–SEP03 and 80 bands (48+32) for JUL02–SEP03 were respectively used as input data for their corresponding networks. The output layer had 5 nodes corresponding 5 'from-to' change classes: 'S to S', 'F to F', 'B to B', 'S to B', and 'B to S'. To find a better ANN structure, we tested various combinations of learning rate (η), momentum coefficient (α) and number of nodes in a hidden layer ($h1$). We tested the three important structure parameters using JUL02–SEP03 training/test data (Table 3). When fixing number of nodes 30 at one hidden layer ($h1$=30), a series of test results from 16 combinations of η and α values (both varied from 0.1 to 0.8) were compared. All OAAs from test samples varied from 77.0 to 97.1% (Fig. 3a) but most combinations over 95%. When using the same input data set, η=0.7 and α=0.2 (dark bar in Fig. 3a), we assessed the effects of $h1$ on OAA calculated from test samples (Fig. 3b). When the hidden-layer nodes was changed from 10 to 70 with various intervals, the highest OAA was 97.1% with 30 nodes at the hidden layer and the lowest OAA=94.0% with 50 nodes. In considering the relatively small variation of OAA values with all testing nodes ($h1$, 10–70) and convenience to design the ANN networks, for the three image-pairs (i.e., JUL02–AUG02, AUG02–SEP03 and JUL02–SEP03), all ANNs use $h1$=30 when original CASI bands are used for input features. However, when using 12 PCs (6 PCs from date 1 CASI image, six PCs from date 2 CASI image) as input features, $h1$=10 was adopted. This is because the number of nodes at the hidden layer could result in highest OAA (98.6%) among the 10 h1 values (h1, 6–20) when fixing η=0.7 and α=0.2 and using JUL02–SEP03 training/test samples. Therefore, we fixed the ANN structure with a 30-node hidden layer for all networks with inputs of original CASI bands and a ten-node hidden layer for all networks with inputs of 12 PCs as well as the learning rate η=0.7 and momentum coefficient α=0.2 in the change detection analysis.

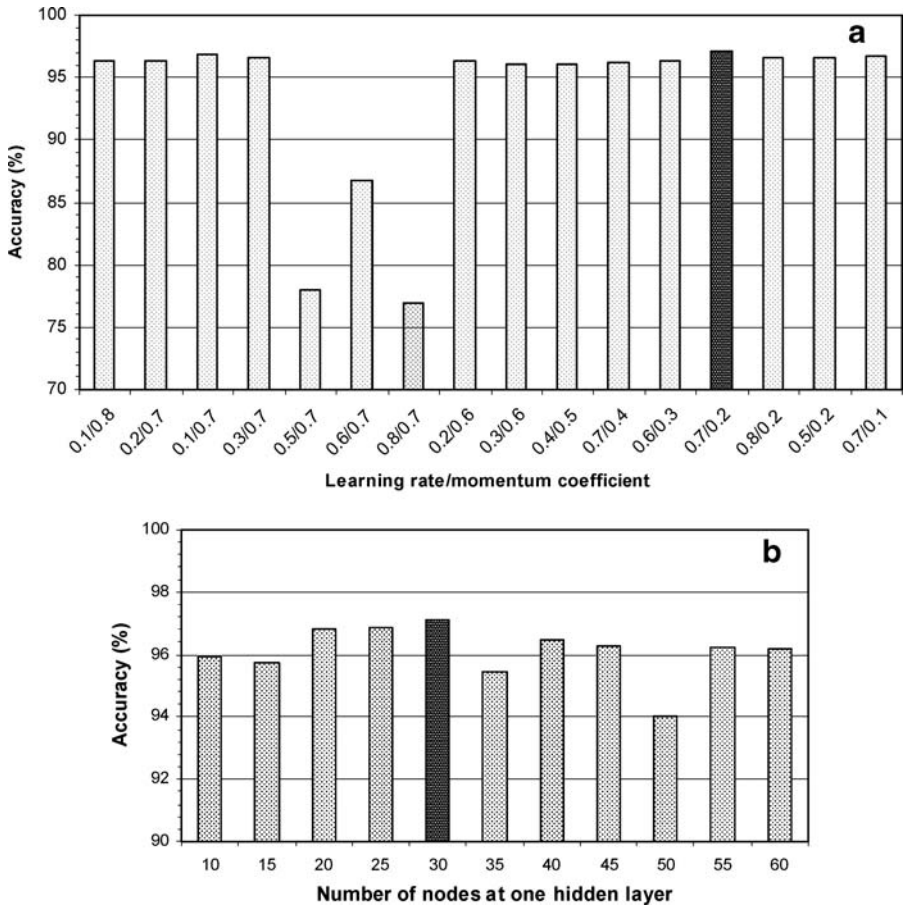

Fig. 3 Determination of some ANN structure parameters tested from a set of training samples (1,036) and a set of test samples (2,072) with maximum number of iterations all set to 10,000. **a** When fixing number of nodes 30 at one hidden layer, testing different eta/alpha combinations; **b** when fixing eta=0.7/alpha=0.2, testing number of nodes at one hidden layer. The training and test samples were extracted from CASI image-pair of JUL02–SEP03

Use of original bands of CASI hyperspectral imagery with ANN

When inputting all original bands of the two-date CASI images into a three-layer ANN architecture (i.e., 84 bands for JUL02–AUG02, 68 input bands for AUG02–SEP03 and 80 bands for JUL02–SEP03), the first part of Table 4 shows classification results calculated from three sets of test samples. From the Table, we can see that the classification accuracies (OAA) of all three image-pairs are higher than 96% and Kappa values are over 0.95. This indicates classifying five 'from-to' change classes using the original CASI bands with ANN classifier is feasible. Figure 4 presents the spatial distribution of the five 'from-to' change classes for the three image pairs: JUL02–AUG02, AUG02–SEP03, and JUL02–SEP03. Generally speaking, the 'S to B' was usually caused by the beetle attack while the 'B to S' was frequently produced by salt cedar growing back after beetle attack or growth (normal phonological change) in the growing season. Visually, it looks that the area of salt cedar growing back is greater than that of salt cedar killed by beetle (more green area than red area) for the JUL02–AUG02 image-pair (Fig. 4a) result, but actually it is not from the statistical results in Table 6. For both AUG02–SEP03 and JUL02–SEP03 image-pairs, it is apparent that the area of salt cedar growing back was smaller than that of salt cedar killed by beetle (more red area than green area). Such a general tendency of salt cedar changed into bare/wildland or vice versa is very similar to those in our previous work (Pu et al. 2007a). Table 5 gives out the validation results of the five 'from-to' change classes with a large sample set. From the first part of the Table, it is clear that the validation results (OAA and Kappa as indicators) are very close to those in Table 4. This further proves the potential of applying ANN to

Table 4 Classification accuracies of five classes calculated from test samples with all original CASI bands or principal component images by ANN or LDA

Change (from-to)	Test set	OAA (%)[a]	Kappa	Variance
NN classification with all CASI bands[b]				
JUL02–>AUG02	Set1	96.78	0.9598	0.000023
	Set2	96.92	0.9616	0.000022
	Set3	96.27	0.9533	0.000026
	Average	96.66	0.9582	0.000024
AUG02–>SEP03	Set1	96.96	0.9620	0.000022
	Set2	95.54	0.9442	0.000032
	Set3	96.39	0.9549	0.000026
	Average	96.30	0.9537	0.000027
JUL02–>SEP03	Set1	97.10	0.9578	0.000025
	Set2	95.90	0.9487	0.000030
	Set3	96.24	0.9529	0.000028
	Average	96.41	0.9531	0.000028
NN classification with principal components[c]				
JUL02–>AUG02	Set1	98.60	0.9825	0.000010
	Set2	98.83	0.9854	0.000008
	Set3	98.65	0.9831	0.000010
	Average	98.69	0.9837	0.000009
AUG02–>SEP03	Set1	98.72	0.9840	0.000009
	Set2	98.86	0.9858	0.000008
	Set3	98.91	0.9864	0.000008
	Average	98.83	0.9854	0.000008
JUL02–>SEP03	Set1	98.60	0.9825	0.000010
	Set2	98.84	0.9855	0.000009
	Set3	98.75	0.9843	0.000009
	Average	98.73	0.9841	0.000009
LDA classification with principal components				
JUL02–>AUG02	Set1	97.25	0.9656	0.000020
	Set2	97.25	0.9656	0.000020
	Set3	96.13	0.9516	0.000027
	Average	96.88	0.9609	0.000022
AUG02–>SEP03	Set1	97.06	0.9632	0.000021
	Set2	97.91	0.9739	0.000015
	Set3	97.44	0.9680	0.000019
	Average	97.47	0.9684	0.000018
JUL02–>SEP03	Set1	97.83	0.9728	0.000016
	Set2	97.83	0.9728	0.000016
	Set3	98.07	0.9759	0.000014
	Average	97.91	0.9738	0.000015

[a] Overall accuracy

[b] With learning rate=0.7, momentum coefficient=0.2, number of nodes in one hidden layer=30

[c] With learning rate=0.7, momentum coefficient=0.2, number of nodes in one hidden layer=10

classify the five 'from-to' change classes. In order to generally know the rates of the five change categories between different periods over the study area, we also calculated the relative percentages of the five change categories as their corresponding change rates for change/no-change detection result of each image pair (Table 6). Since the purpose of this study is mainly focusing on the characterization of the two important 'from-to' categories: 'S to B' and 'B to S,' from the table, the change rates of 'S to B' for all three image-

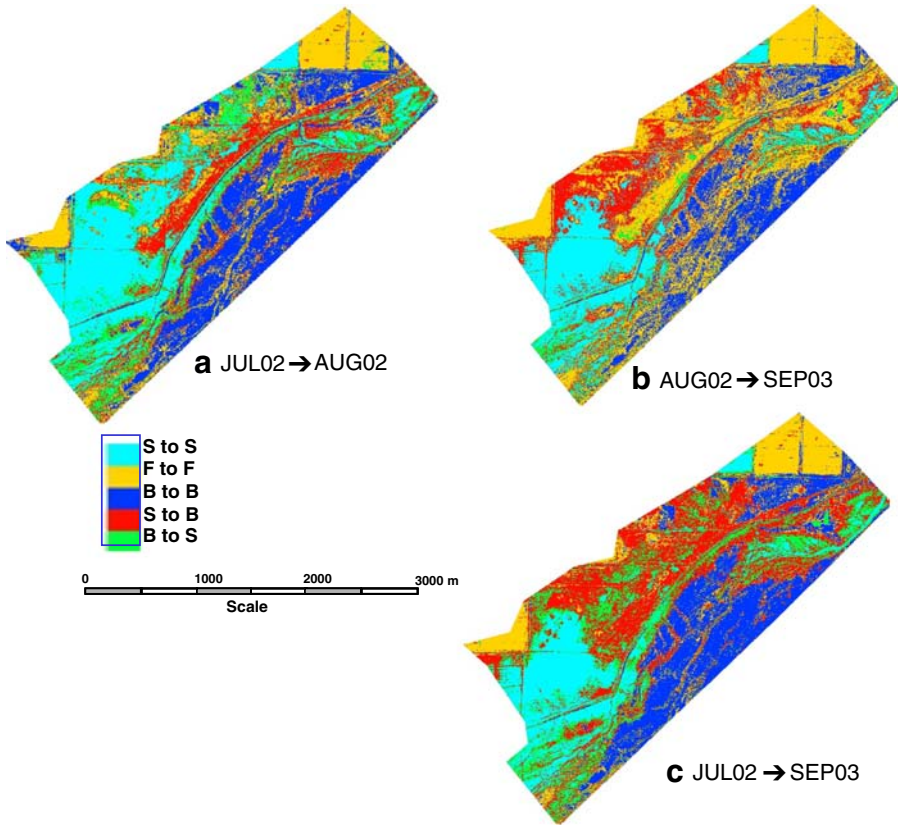

Fig. 4 Change detection resultant maps produced by ANN with all original CASI bands from JUL01 to AUG02 (**a**), from AUG02 to SEP03 (**b**), and from JUL02 to SEP03 (**c**). In legend, 'S to S', 'F to F', and 'B to B' represent no-changes of salt cedar, farmland and bare/wildland, respectively; 'S to B' means salt cedar changed to bare/wildland while 'B to S' means bare/wildland changed to salt cedar

pairs are higher than those of 'B to S' except a small difference for JUL02–AUG02 image pair between the two change rates.

Use of CASI PCA transformed data with ANN

Figure 5 presents the classification results of the 5 'from-to' change classes generated using 12 PCs of CASI image-pair with ANN. The area of 'S to B' was smaller than the that of 'B to S' for JUL02–AUG02 image-pair, but for both AUG02–SEP03 and JUL02–SEP03 image-pairs, more area of 'S to B' happed due to beetle attack to salt cedar. The statistics of change rates in Table 6 also prove this point. The properties of change rates for the two interesting categories can be discussed with the same reasons as those in the above subsection. The middle part of Table 4 shows the classification accuracies and Kappa values that indicate OAA >98% and Kappa >0.98 for the three test sets. Accordingly, the middle part of Table 5 lists the classification accuracies and Kappa values that are all similar to those in Table 4. In general, the results in both figure (Fig. 5) and tables (Tables 4 and 5) demonstrate the successful application of ANN in change detection with the direct multi-date image classification. Due to significantly low dimension of 12 PCs compared to original bands, the computation efficiency was greatly increased with input of CASI PCA transformation data.

Use of CASI PCA transformed data with LDA

With exactly the same inputs of 12 PCs as for ANN for the three image-pairs, Fig. 6 shows the spatial distributions of the five 'from-to' land cover change classes produced by the LDA. Generally, from the figure, the distributions of 'S to B' and 'B to S' for the three image-pairs have a similar tendency of distribution to those from Fig. 5 (also see Table 6). The low parts in Tables 4 and 5 also show that the LDA classifier applied to the five 'from-to' land cover change classification is successful although the values of the two accuracy assessment indicators: OAA and Kappa, are slightly lower than those by ANN. Due to the data dimension too high for original bands of multi-date CASI images as inputs that might lead to LDA not

Table 5 Confusion matrices and Kappa values, calculated from validation data sets for the three-pair change detection images, with all original CASI bands or principal component images by ANN or LDA

	Reference							
		SS	FF	BB	SB	BS	User's accu(%)	Kappa
NN classified with all original CASI bands								
JUL02–>AUG02	SS	554,727	0	147	20	683	99.85	0.9487
	FF	0	231,059	9,669	488	14	95.78	
Classified	BB	0	5,081	415,624	442	27	98.68	
	SB	0	4,920	14,064	18,788	55	49.67	
	BS	8,448	887	0	33	40,175	81.09	
	Producer's accu(%)	98.50	95.50	94.57	95.03	98.10	OAA=96.55	
AUG02–>SEP03	SS	416,654	245	0	0	0	99.94	0.9437
	FF	0	202,011	629	74	44	99.63	
Classified	BB	0	39,130	313,598	0	0	88.91	
	SB	0	2,935	315	74,089	0	95.80	
	BS	417	245	0	0	43,733	98.51	
	Producer's accu(%)	99.90	82.60	99.70	99.90	99.90	OAA=95.98	
JUL02–>SEP03	SS	352,222	0	0	0	525	99.85	0.9460
	FF	0	226,931	3,918	663	8	98.02	
Classified	BB	0	11,157	391,131	765	42	97.03	
	SB	0	3,719	10,268	24,045	8	63.21	
	BS	7,555	728	0	25	24,827	74.93	
	Producer's accu(%)	97.90	93.57	96.50	94.30	97.70	OAA=96.28	
NN classified with principal components								
JUL02–>AUG02	SS	562,424	0	147	7	0	99.97	0.9763
	FF	0	235,979	10,109	0	164	95.83	
Classified	BB	0	4,436	426,026	86	68	98.93	
	SB	563	242	1,319	19,658	41	90.08	
	BS	188	1,290	1,905	20	40,680	100.00	
	Producer's accu(%)	99.87	97.53	96.93	99.43	99.33	OAA=98.42	
AUG02–>SEP03	SS	416,932	0	0	25	58	99.98	0.9822
	FF	0	237,880	6,081	49	263	97.38	

Classified	BB	0	5,380	307,937	25	117	98.24	
	SB	0	978	419	74,064	15	98.13	
	BS	139	326	105	0	43,325	98.70	
	Producer's accu(%)	99.97	97.27	97.90	99.87	98.97	OAA=98.72	
JUL02–>SEP03	SS	359,657	0	0	17	8	99.99	0.9771
	FF	0	236,551	8,647	25	42	96.45	
Classified	BB	0	5,255	395,184	153	68	98.63	
	SB	0	162	676	25,269	25	96.70	
	BS	120	566	811	34	25,267	94.29	
	Producer's accu(%)	99.97	97.53	97.50	99.10	99.43	OAA=98.43	
LDA classified with principal components								
JUL02–>AUG02	SS	562,987	0	0	0	96	99.98	0.9527
	FF	0	237,995	30,033	244	41	88.70	
Classified	BB	0	2,903	403,172	376	123	99.16	
	SB	0	81	4,542	19,151	14	80.51	
	BS	188	968	1,758	0	40,680	93.32	
	Producer's accu(%)	99.97	98.37	91.73	96.87	99.33	OAA=96.83	
AUG02–>SEP03	SS	417,071	0	0	0	131	99.97	0.9664
	FF	0	239,266	19,082	74	263	92.49	
Classified	BB	0	4,565	295,145	470	700	98.09	
	SB	0	489	315	73,619	44	98.86	
	BS	0	245	0	0	42,639	99.43	
	Producer's accu(%)	100.00	97.83	93.83	99.27	97.40	OAA=97.59	
JUL02–>SEP03	SS	359,417	0	0	0	42	99.99	0.9737
	FF	0	234,773	9,052	93	59	96.23	
Classified	BB	0	7,438	395,860	756	500	97.85	
	SB	0	0	405	24,648	34	98.25	
	BS	360	323	0	0	24,776	97.32	
	Producer's accu(%)	99.90	96.80	97.67	96.67	97.50	OAA=98.20	

SS Change from salt cedar to salt cedar, *FF* change from farmland to farmland, *BB* change from bare/wildland to bare/wildland, *SB* change from salt cedar to bare/wildland, *BS* change from bare/wildland to salt cedar, *OAA* overall accuracy (%)

Table 6 Rates (%) of changes for different change categories and periods in the study area

Change category	JUL02–>AUG02			AUG02–>SEP03			JUL02–>SEP03		
	ALL-ANN	PC-ANN	PC-LDA	ALL-ANN	PC-ANN	PC-LDA	ALL-ANN	PC-ANN	PC-LDA
Salt cedar–>salt cedar	24.32	19.13	20.39	19.99	14.91	16.80	15.55	13.26	15.54
Farmland–>farmland	18.57	25.06	36.09	34.23	24.05	30.09	14.11	23.26	21.43
Bare/wild–>bare/wild	22.79	28.64	22.67	17.11	30.77	24.83	22.87	34.92	39.04
Salt cedar–>bare/wild	18.04	10.98	6.17	21.26	18.35	17.75	29.12	14.75	12.74
Bare/wild–>salt cedar	16.28	16.19	14.68	7.41	11.92	10.53	18.35	13.81	11.25
Sum	100.00	100.00	100.00	100.00	100.00	100.00	100.00	100.00	100.00

The rates were derived from the resultant maps produced by ANN with all CASI bands and PCs and by LAD with PCs (Figs. 4, 5 and 6)
ALL-ANN ANN method with all original CASI bands, *PC-ANN or PC-LDA* ANN or LDA method with 12 PCs

working properly, we classified the five 'from-to' change classes with the LDA only using the CASI PCA transformation data (i.e., 12 PCs for each image-pair).

Comparisons

The purpose of this study for detecting and monitoring the invasive species change was to test the feasibility of the direct multi-date image classification method and ANN algorithm as a classifier with CASI hyperspectral data. To this end, we also tested a traditional method: Linear discriminant analysis (LDA) for evaluating the performance of ANN. When using the ANN as a classifier, the comparison of results of the five 'from-to' change/no-change classes, produced with inputs of either all original bands or 12 PCs of CASI data, indicate that the lower dimension of 12 PCs images has produced higher accuracies and

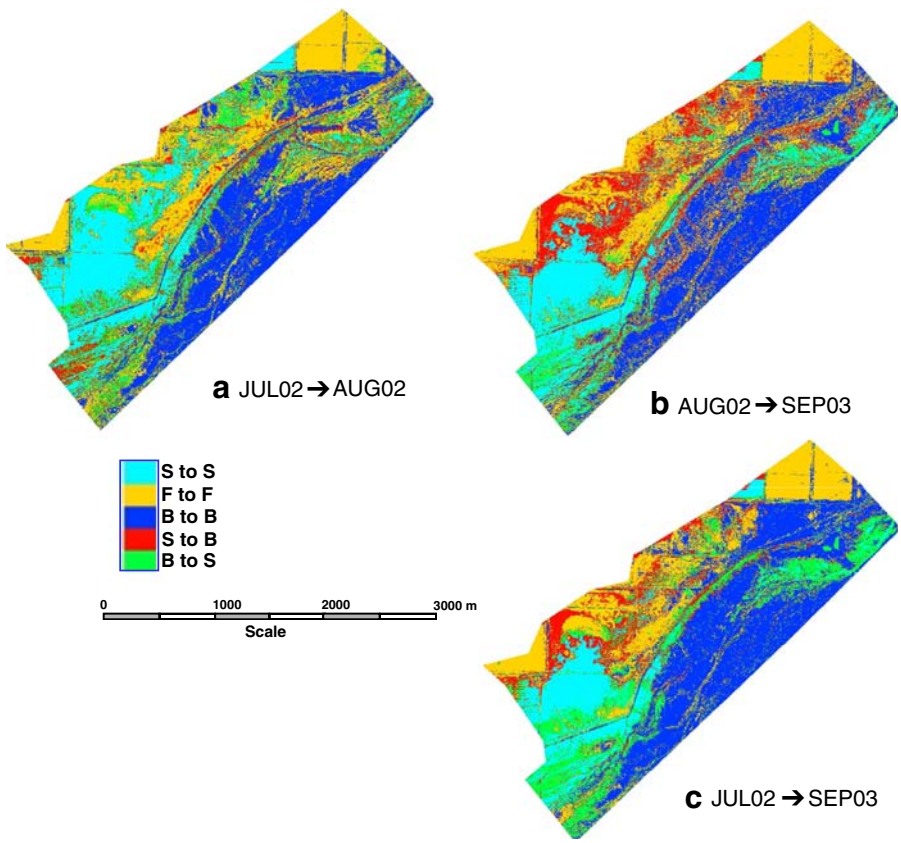

Fig. 5 Change detection resultant maps produced by ANN with principal components extracted from the CASI data from JUL01 to AUG02 (**a**), from AUG02 to SEP03 (**b**), and from JUL02 to SEP03 (**c**). In legend, 'S to S', 'F to F', and 'B to B' represent no-changes of salt cedar, farmland and bare/wildland, respectively; 'S to B' means salt cedar changed to bare/wildland while 'B to S' means bare/wildland changed to salt cedar

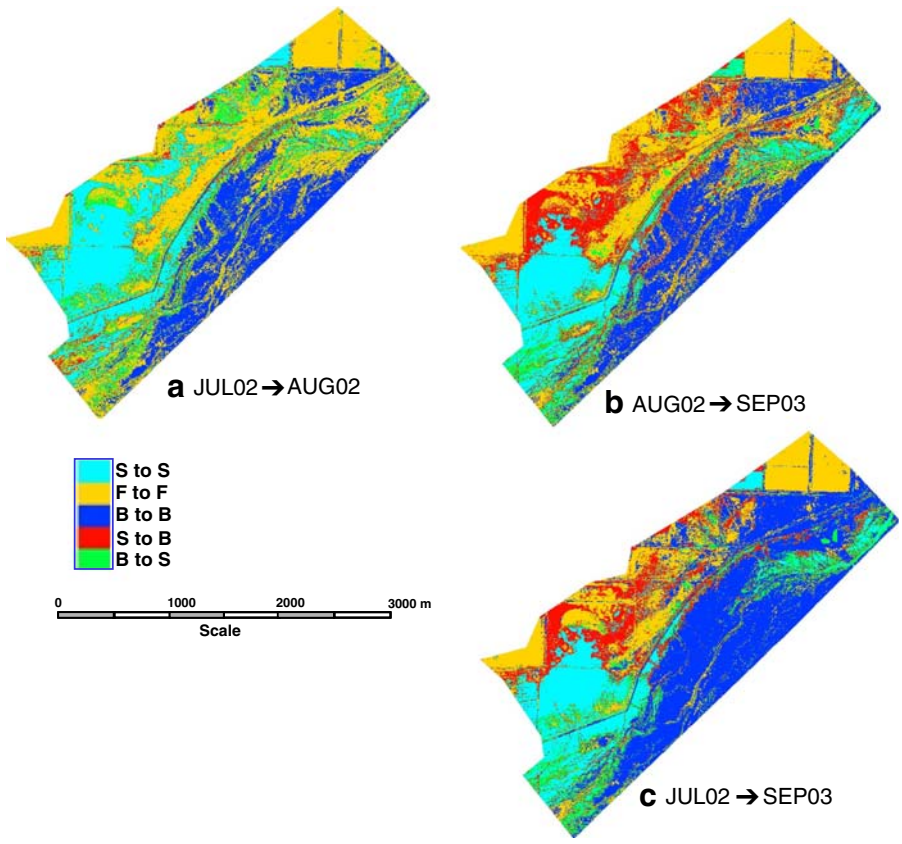

Fig. 6 Change/no-detection resultant maps produced by LDA with principal components extracted from the CASI data from JUL01 to AUG02 (**a**), from AUG02 to SEP03 (**b**), and from JUL02 to SEP03 (**c**). In legend, 'S to S', 'F to F', and 'B to B' represent no-changes of salt cedar, farmland and bare/wildland, respectively; 'S to B' means salt cedar changed to bare/wildland while 'B to S' means bare/wildland changed to salt cedar

Kappa values than those with the higher dimension of original CASI data. The higher accuracies generated with the former low dimension data were OAA >98.7% from test samples and OAA >98.4% from validation samples and Kappa values >0.98 from the test samples and >0.97 from the validation samples compared to corresponding accuracies OAA, >96.3 and >96.0% and Kappa values, >0.95 and 0.94 with the latter high dimension CASI data (Tables 4 and 5). This may be that the 12 PC-images as inputs of the ANN have efficiently reduced the effect of redundancy of all original CASI band data on final classification result. From Table 6, it is reasonable for rates of the three no-change categories: 'S to S', 'F to F' and 'B to B' because their rates are relatively unchanged among the three image-pairs. The Z-statistic test results (Table 7), calculated from test samples, indicate that difference of Kappa between the 12 PCs and all original CASI bands as inputs is significant at 0.99 confidence level. When checking distributions of 'S to B' and 'B to S' change classes over the classification maps (Figs. 4 vs 5), it is obvious that distribution area of 'S to B' class is too much on maps created with original CASI bands

Table 7 Z-statistic test calculated from Kappa-variance of classification results of test samples, generated with all original CASI bands or principal component images by ANN or LDA

Change (from-to)	JUL02–>AUG02	AUG02–>SEP03	JUL02–>SEP03
Z [ANN(all bands vs PCs)]	4.439[a]	5.358[a]	5.096[a]
Z [ANN(PCs) vs LDA(PCs)]	4.095[a]	3.334[a]	2.102[b]

$Z = \frac{|k_1 - k_2|}{\sqrt{v_1 + v_2}}$ where, k_1 and k_2 are kappa vappa values of corresponding input feature 1 and input feature 2, respectively, and v_1 and v_2 are corresponding variances.

[a] Difference between classification accuracies by two sets of input features is significant at 0.99 confidence level.

[b] Difference between classification accuracies by two sets of input features is significant at 0.95 confidence level.

(Fig. 4), especially for maps of JUL02–AUG02 (Fig. 4a) and JUL02–SEP03 (Fig. 4c) compared to the pseudo-color composite images (Fig. 2). The statistics from Table 6 also support this point. Therefore, the visual comparison results of spatial distributions of 'S to B' and 'B to S' areas in Figs. 4 and 5 and the statistics from Table 6 seem also indicating that the 'from-to' change classification results with the 12 PCs are better than those with all original CASI bands.

When considering the results of the five 'from-to' change/no-change classes produced by the two classifiers: ANN and LDA with the same inputs of 12 PCs, we can find that the LDA classifier has produced relative lower accuracies and Kappa values than those by the ANN although both are high. The lower accuracies generated using the LDA were OAA >96.9% from test samples and OAA >96.8% from validation samples and Kappa values >0.96 from the test samples and >0.95 from the validation samples compared to corresponding accuracies OAA, >98.7 and >98.4% and Kappa values, >0.98 and 0.97 using the ANN (Tables 4 and 5). The Z-statistic test results (Table 7) show that difference of Kappa between ANN and LDA is significant at a 0.99 confidence level for JUL02–AUG02 and AUG02–SEP03 image-pairs and at a 0.95 confidence level for JUL02–SEP03 image-pair. When checking distributions of 'S to B' and 'B to S' change classes between the classification maps produced with ANN (Fig. 5) and with LCD (Fig. 6), very similar distribution patterns between can be found. This might mainly be related to use of the same 12 PCs as inputs. However, if based on the test and validation results (Tables 4 and 5) and relatively unchanged rates of the three no-change categories among the three periods, the ANN clearly outperforms the LDA in this 'from-to' change detection with the direct multi-date data classification method.

Discussion and conclusions

The direct multi-date image classification method or spectral-temporal combined change detection method used in this analysis is less frequently used in practice due to the difficulty in identifying and labeling change trajectories (Lu et al. 2004). It is true if adopting an unsupervised method due to a large number of 'from-to' change classes that could be exponentially greater than those in a single data classification. However, if using a supervised classifier, such as ANN or LDA used in this analysis, and training/test samples being available for historical image data, this method is a direct approach to classify 'from-to' change classes valid in a specific study area and interested for a change detection purpose. This method also is easy to label the change trajectories if you can define 'from-to' change classes first on your multitemporal image set. Thus, this method is capable of giving out the complete change information about land cover change. For example, in this study, we referred to the historical digital photos taken before acquiring the multi-date CASI imagery to help delineate the 'from' classes at time 1 and 'to' classes at time 2 then based on their same location to determine the nature of 'from-to' change classes. In practice, many 'from-to' classes do not appear in a specific study area. So actual number of 'from-to' change classes is not as large as that theoretically calculated. For instance, in our case, we considered only five 'from-to' change classes and in Nemmour and Chibani (2006) case, they only used eight classes. Therefore, based on our experimental results and other researchers' work (e.g., Liu and Lathrop 2002; Nemmour and Chibani 2006), this direct multi-date image classification method is effective in change detection if adopting a supervised classifier and training/test data available for historical image data.

This is first time to test the direct multi-date hyperspectral image classification in change detection. Due to the high dimension of hyperspectral data, direct use of original bands of multi-date image should consider the computation cost besides the classification accuracy. Therefore, a traditional PCA transformation technique was conducted to the original CASI data to lower the dimension of the hyperspectral data. In this PCA analysis, the PCA was just used as a regular enhancement tool to individual images without considering the land cover variation information linked to 'from-to' change classes. With the same classifier ANN, the comparison results of the 5 'from-to' change classes, produced with all original CASI bands and 12 PCs, indicate that classification accuracies and kappa values derived from the 12 PCs as inputs were all better than those derived from all original bands. This may be that PCA transformation reduces the redundancy of raw data, which would benefit classification of 'from-to' change classes. Therefore, in this study, the PCA pre-processing

to original CASI data not only lowered the computation cost but improved the change detection accuracy as well.

Compared to the results produced using the LDA, the ANN generated better change detection results when considering the same input of 12 PCs of the CASI data. This may be thanks to the non-linear property of the ANN algorithm that can catch more 'from-to' change class information than the LDA can because we believe such land cover change, either continuously or abruptly, is non-linear change. Another cause may be that some land cover types are not normally distributed. For example, when salt cedar plant is partially killed by the beetle, its distribution of radiometric values derived from the image data may not be normal although this issue is not proved yet so far. As we know, the ANN can handle data without a certain distribution of analysis data. To this end, our experimental results partially prove the two presumptions. Some literature, e.g., Lu et al. (2004) and Nemmour and Chibani (2006), has confirmed this point.

In this study, a direct multi-date image classification method was applied in invasive species (salt cedar) change detection in the study area of Lovelock, Nevada. For this case, we have examined and compared two types of hyperspectral CASI input data and two classifiers for mapping and monitoring the salt cedar change in the study area. The two types of input data are all two-date original CASI bands and 12 PCs derived from the two-date images. The two classifiers are ANN and LDA. The three image-pairs (JUL02–AUG02, AUG02–SEP03 and JUL02–SEP03) of airborne hyperspectral CASI data were used in this experiment of land cover change detection. Based on the experimental results, we can conclude that (1) the direct multitemporal image classification applied in land cover change detection is feasible either with original CASI bands or principal component images (PCs) but a better accuracy was obtained from the CASI PCA transformed data; (2) with the same inputs of 12 PCs, the ANN outperforms the LDA due to the ANN's non-linear property and ability of handling data without a prerequisite of a certain distribution of the analysis data. Our ongoing work will focus on the ANN's ability of predicting land cover continuous change information (Bruzzone et al. 1999; Dai and Khorranm 1999; Gopal and Woodcock 1996; Liu and Lathrop 2002; Nemmour and Chibani 2006) to estimate magnitude of salt cedar gradually killed or damaged by beetle in our study area.

Acknowledgements We thank USDA for providing us with CASI imagery.

References

Abuelgasim, A. A., Ross, W. D., Gopal, S., & Woodcock, C. E. (1999). Change detection using adaptive fuzzy neural networks: Environmental damage assessment after the Gulf War. *Remote Sensing of Environment, 70,* 208–223.

Aplin, P. (2006). On scales and dynamics in observing the environment. *International Journal of Remote Sensing, 27* (11), 2123–2140.

Bruzzone, L., Prieto, D. F., & Serpico, S. B. (1999). A neural-statistical approach to multitemporal and multisource remote-sensing image classification. *IEEE Transactions on Geoscience and remote Sensing, 31,* 511–515.

Civco, D. L., Hurd, J. D., & Wilson, E. H. (2002). A comparison of land use and land cover change detection methods. In *Proceedings of ASPRS Annual Convention* (p. 12). Washington, DC: ASPRS, 22–26 April 2002.

Congalton, R. G., & Mead, R. A. (1983). A quantitative method to test for consistency and correctness in photointerpretation, *Photogrammetric Engineering and Remote Sensing, 49*(1), 69–74.

Congalton, R. G., Oderwald, R. G., & Mead, R. A. (1983). Assessing Landsat classification accuracy using discrete multivariate statistical techniques. *Photogrammetric Engineering and Remote Sensing, 49*(12), 1671–1678.

Coppin, P., Jonckheere, I., Nackaerts, K., Muys, B., & Lambin, E. (2004). Digital change detection methods in ecosystem monitoring: A review. *International Journal of Remote Sensing, 25*(9), 1565–1596.

Dai, X. L., & Khorranm, S. (1999). Remotely sensed change detection based on artificial neural networks. *Photogrammetric Engineering and Remote Sensing, 65,* 1187–1194.

Foody, G. M. (2002). Status of land cover classification accuracy assessment. *Remote Sensing of Environment, 80,* 185–201.

Foody, G. M., McCulloch, M. B., & Yates, W. B. (1995). Classification of remotely sensed data by an artificial neural network: Issue related to training data characteristics. *Photogrammetric Engineering and Remote Sensing, 61,* 391–401.

Fung, T., & LeDrew, E. (1988). The determination of optimal threshold levels for change detection using various accuracy indices. *Photogrammetric Engineering and Remote Sensing, 54*(10), 1449–1454.

Gong, P., Pu, R. & Yu, B. (1997). Conifer species recognition: An exploratory analysis of in situ hyperspectral data. *Remote Sensing of Environment, 62,* 189–200.

Gong, P., & Xu, B. (2004). *Remote sensing of forests over time-change types, methods, and opportunities* (pp. 301–333). The Netherlands: Kluwer.

Gopal, S., & Woodcock, C. E. (1996). Remote sensing of forest change using artificial neural networks. *IEEE Transactions on Geoscience and Remote Sensing, 34,* 398–404.

Hayes, D. J., & Sader, S. A. (2001). Comparison of change-detection techniques for monitoring tropical forest clearing and vegetation regrowth in a time series. *Photogrammetric Engineering and Remote Sensing, 67*(9), 1067–1075.

Jackson, R. B., Banner, J. L., Jobbagy, E. G., Pockman, W. T., & Wall, D. H. (2002). Ecosystem carbon loss with woody plant invasive pf grasslands. *Nature, 418,* 623–626.

Johnson, W., Davison, J., Young, J., & Kadrmas, T. (2005). Managing Saltcedar, http://www.unce.unr.edu/publications/FS02/FS0293.pdf, access on May 15, 2005. University of Nevada, Reno

Khan, S. D. (2005). Urban development and flooding in Houston Texas, inferences from remote sensing data using neural network technique. *Environmental Geology, 47,* 1120–1127.

Lass, L. W., Thill, D. C., Shafii, B., & Prather, T. S. (2002). Detecting spotted knapweed (*Centaurea maculosa*) with hyperspectral remote sensing technology. *Weed Technology, 16*(2), 426–432.

Liu, X., & Lathrop, R. G. Jr. (2002). Urban change detection based on an artificial neural network. *International Journal of Remote Sensing, 23,* 2513–2518.

Lu, D., Mausel, P., Brondizio, E., & Moran, E. (2004). Change detection techniques. *International Journal of Remote Sensing, 25*(12), 2365–2407.

Mack, R. N., Simberloff, D., Lonsdale, W. M., Evans, H., Clout, M., & Bazzaz, F. (2000). Biotic invasions: causes, epidemiology, global consequences and control. *Ecological Application, 10,* 689–710.

Miao, X., Gong, P., Swope, S., Pu, R., Carruthers, R., Anderson, G. L. et al. (2006). Estimation of yellow starthistle abundance through CASI-2 hyperspectral imagery using linear spectral mixture models. *Remote Sensing of Environment, 101*(3), 329–341.

Nemmour, H., & Chibani, Y. (2006). Fuzzy neural network architecture for change detection in remotely sensed imagery. *International Journal of Remote Sensing, 27*(4), 705–717.

Pao, Y. (1989). *Adaptive pattern recognition and neural networks*. New York: Addison and Wesley.

Pu, R., Gong, P., Tian, Y., Miao, X., Carruthers, R. I., & Anderson, G. L. (2007a). Using classification and NDVI differencing methods for monitoring sparse vegetation coverage: A case study of saltcedar in Nevada, USA. *International Journal of Remote Sensing* (in press)

Pu, R., Kelly, M., Anderson, G. L., & Gong, P. (2007b). Using CASI hyperspectral imagery to detect mortality and vegetation stress associated with a new hardwood forest disease. *Photogrammetric Engineering and Remote Sensing* (in press).

Rumelhart, D. E., Hinton, G. E., & Williams, R. J. (1986). Learning internal representations by error propagation. In D. E Rumelhart & J. L. McCelland (Eds.) *Parallel distributed processing-explorations in the microstructure of cognition, vol. 1* (pp. 318–362). Cambridge, MA: MIT Press.

SAS Institute Inc. (1991). *SAS/STA User's Guide, Release 6.03 Edition* (p. 1028). Gary, NC: SAS Institute Inc., USA.

Seto, K. C., & Liu, W. (2003). Comparing ARTMAP neural network with the maximum-likelihood classifier for detecting urban change. *Photogrammetric Engineering and Remote Sensing, 69*(9), 981–990.

Simberloff, D. (2001). Biological invasions: How are they affecting us and what can we do about them? *Western North American Naturalist, 61,* 308–315.

Sunar Erbek, F., Özkan, C., & Taberner, M. (2004). Comparison of maximum likelihood classification method with supervised artificial neural network algorithms for land use activities. *International Journal of Remote Sensing, 25*(9), 1733–1748.

Underwood, E., Ustin, S., & DiPietro, D. (2003). Mapping nonnative plants using hyperspectral imagery. *Remote Sensing of Environment, 86*(2), 150–161.

USDA ARS (2005). Saltcedar, *Tamarix* spp.: An emerging success. Retrieved May 15, 2005 from http://www.invasivespecies.gov/docs/ars/issssaltcedar.pdf.

Ustin, S. L., Scheer, G., DiPietro, D., Underwood, E., & Olmstead, K. (2001). Hyperspectral remote sensing for invasive species detection and mapping. *Abstracts of Papers of the American Chemical Society, 221,* U50.

van Aardt, J. A. N., & Wynne, R. H. (2001). Spectral separability among six southern tree species. *Photogrammetric Engineering and Remote Sensing, 67,* 1367–1375.